

Fig. 31-8.1-0 wind field geometry for Case III and special output points

#9

1.5 -

CASE 3

DX : 40 KM, DT : 1.0 HOUR
 IMAX=26 : JMAX=26
 X EXTENT:0-1000 KM
 Y EXTENT:0-1000 KM

DIR. OF WIND : SOUTHWEST
 VEL. OF WIND : 20 M/SEC

TIME 72 HOURS
 T* IS 2972764.

CONTOURS OF SCALED E
 ON INTERVAL 0.1

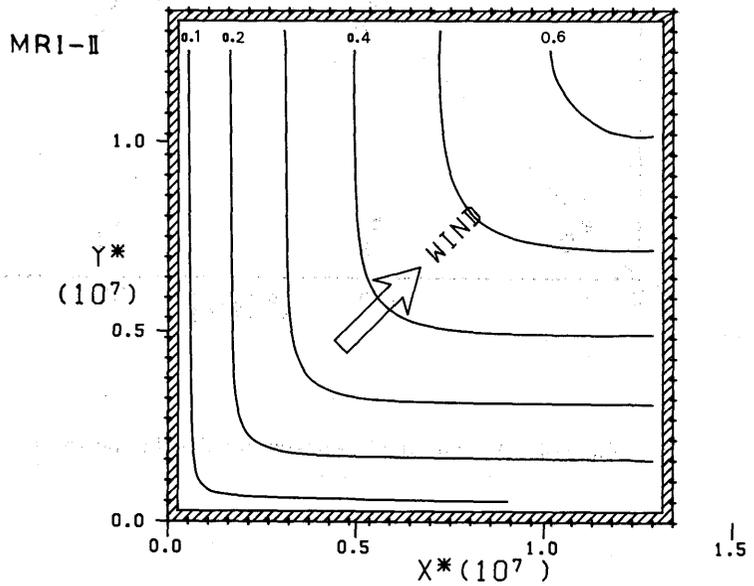
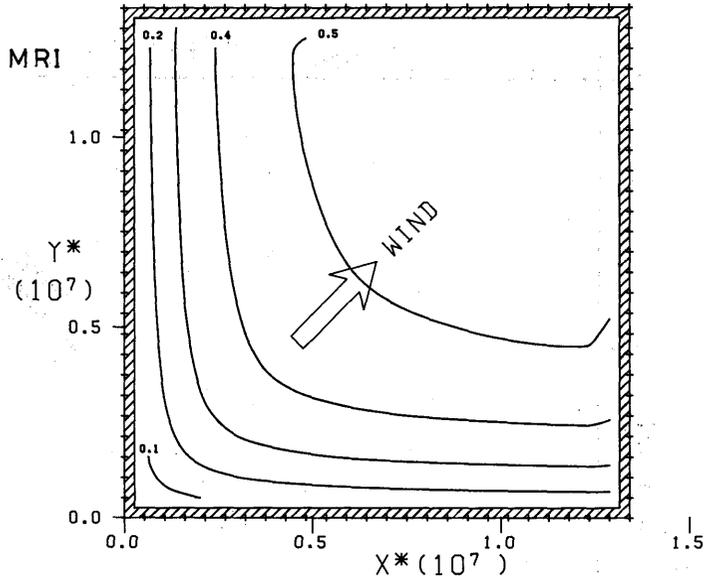


Fig. 32-0-11 contours of E/E_{PM} vs. X^* and Y^*

#10

1.5 -

CASE 3

DX : 40 KM, DT : 1.0 HOUR
 IMAX=26 : JMAX=26
 X EXTENT:0-1000 KM
 Y EXTENT:0-1000 KM

DIR. OF WIND : SOUTHWEST
 VEL. OF WIND : 20 M/SEC

TIME 72 HOURS
 T* IS 2972764.

CONTOURS OF \bar{f}/f_{PM}
 ON INTERVAL 0.1 FOR
 RANGE 1 TO 2, 0.5 FOR >2

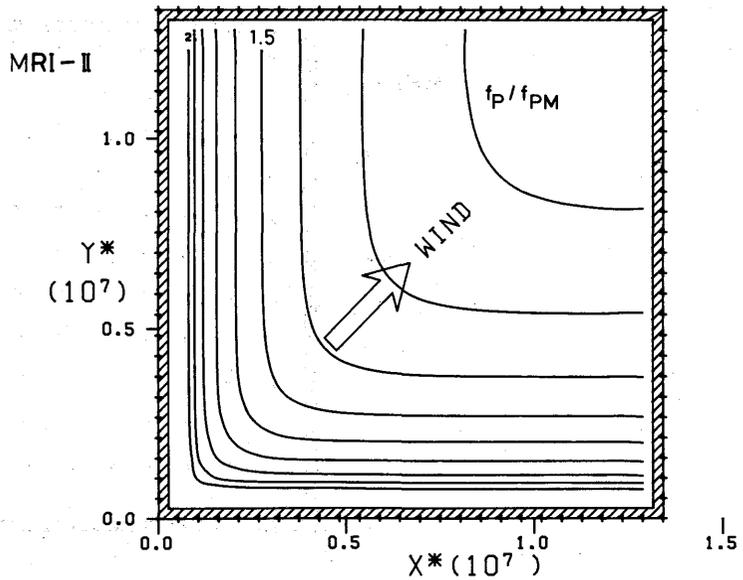
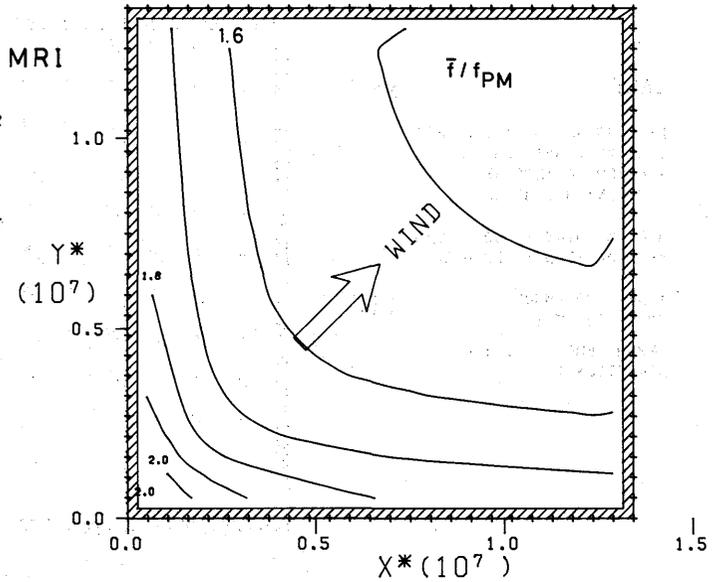


Fig. 33-8.2-12 contours of f_P/f_{PM} vs. X^* and Y^*

#11

CASE 3

DX : 40 KM. DT : 1.0 HOUR
 IMAX=26 : JMAX=26
 X EXTENT:0-1000 KM
 Y EXTENT:0-1000 KM

DIR. OF WIND : SOUTHWEST
 VEL. OF WIND : 20 M/SEC

TIME : 72 HOURS
 T* IS 2972764.

ARROW LENGTH : E/E_{PM}
 DIRECTION= θ

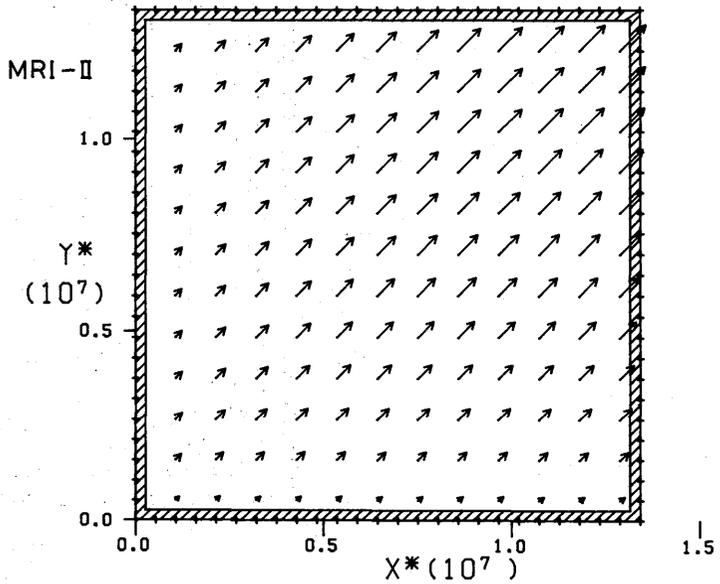
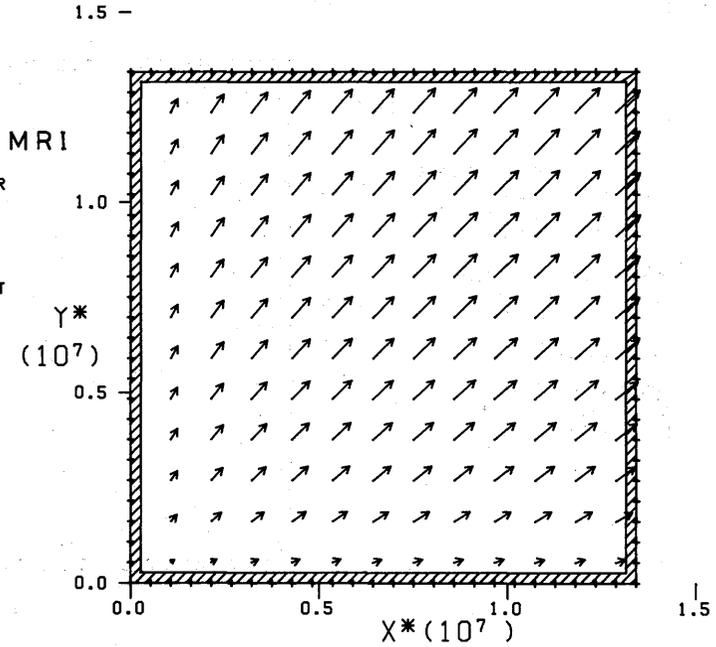


Fig. 34-8.3-13 cluster diagram of E/E_{PM} and θ vs. X^* and Y^*

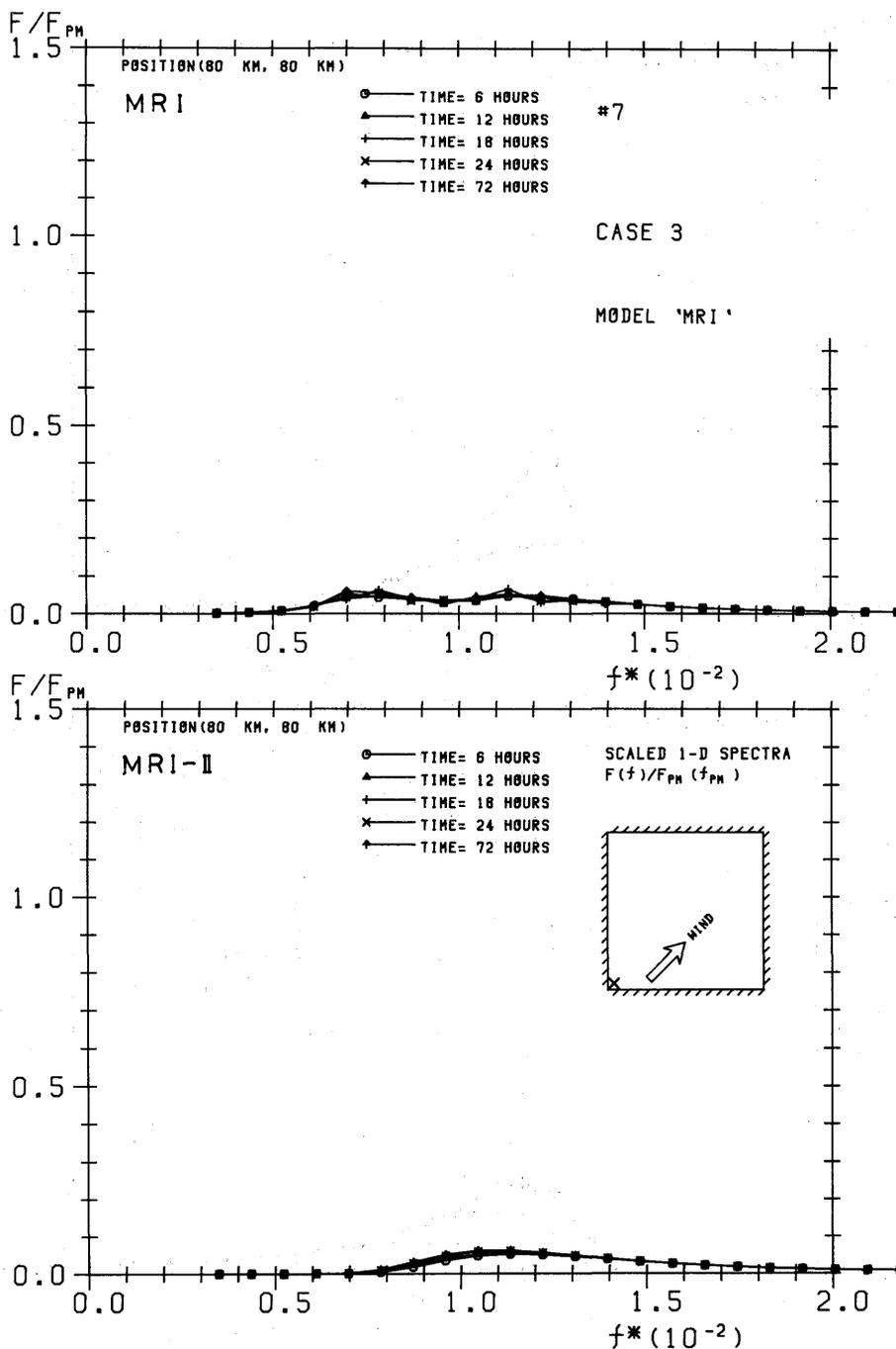


Fig. 35-0-0 scaled 1-D spectrum $F(f)/F_{PM}(f_{PM})$ vs. f^* for $T=6, 12, 24, 72$ and point (80,80)

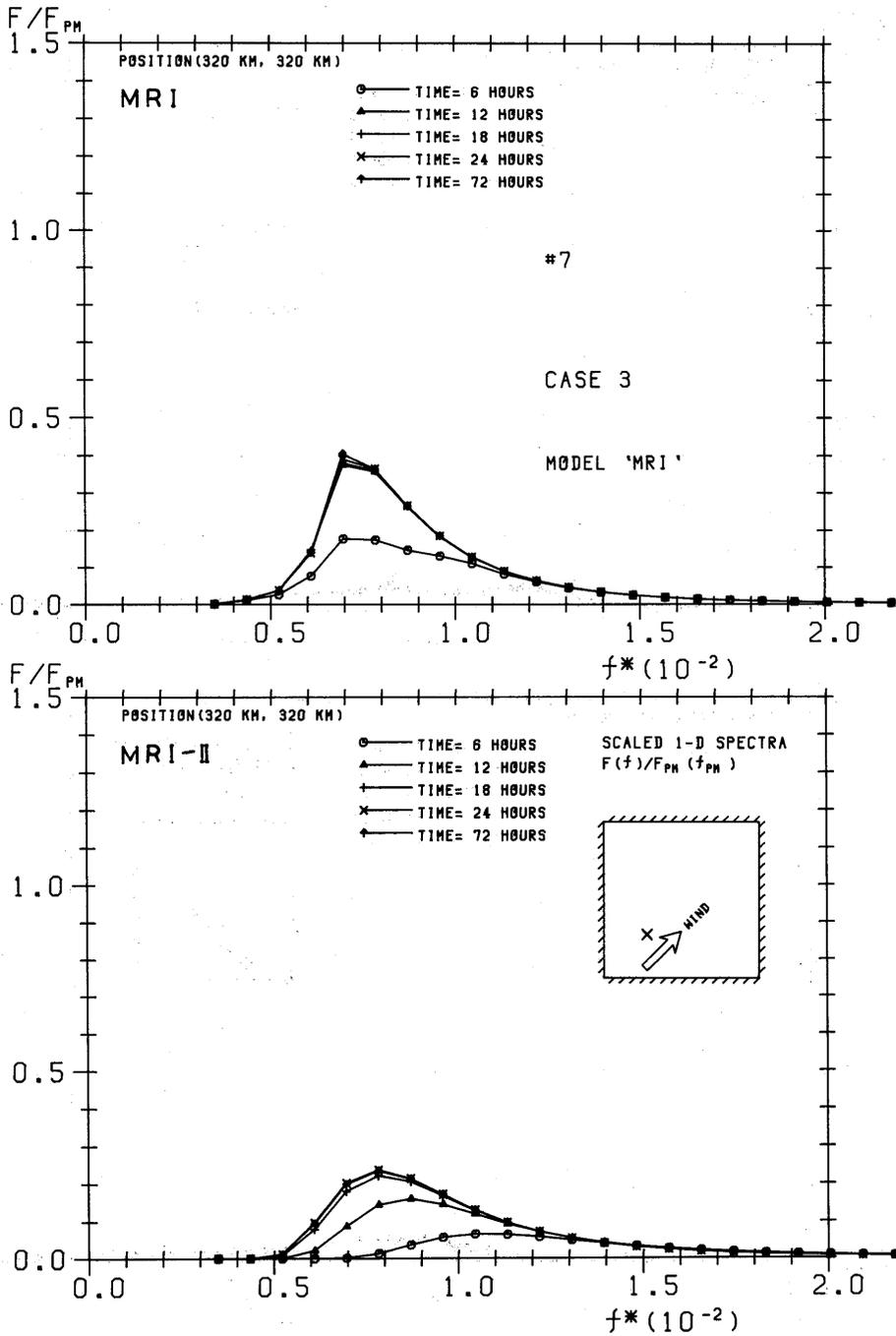


Fig. 36-0-0 scaled 1-D spectrum $F(f)/F_{PM}(f_{PM})$ vs. f^* for $T=6, 12, 24, 72$ and point (320,320)

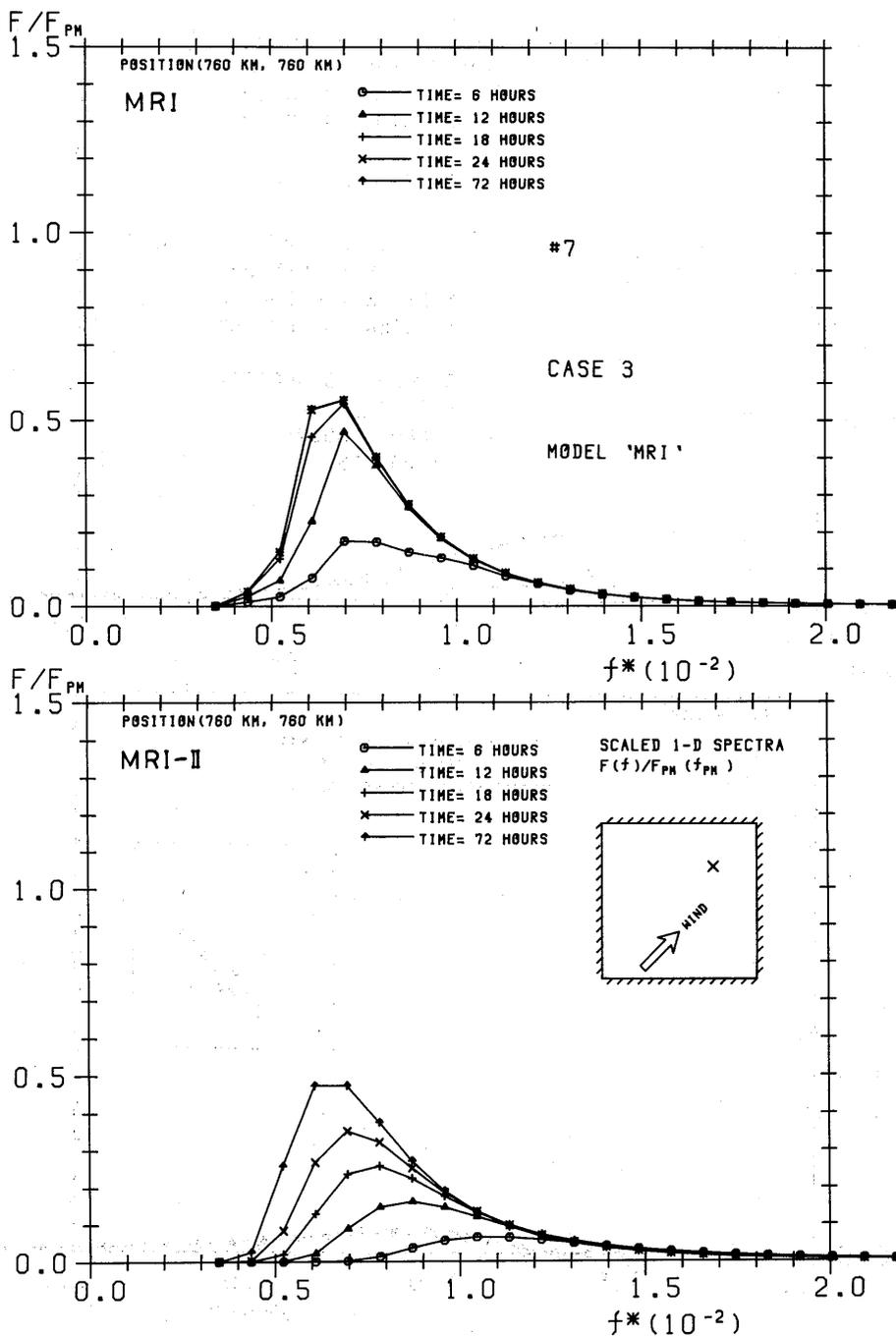


Fig. 37-0-0 scaled 1-D spectrum $F(f)/F_{PM}(f_{PM})$ vs. f^* for $T=6, 12, 24, 72$ and point (760,760)

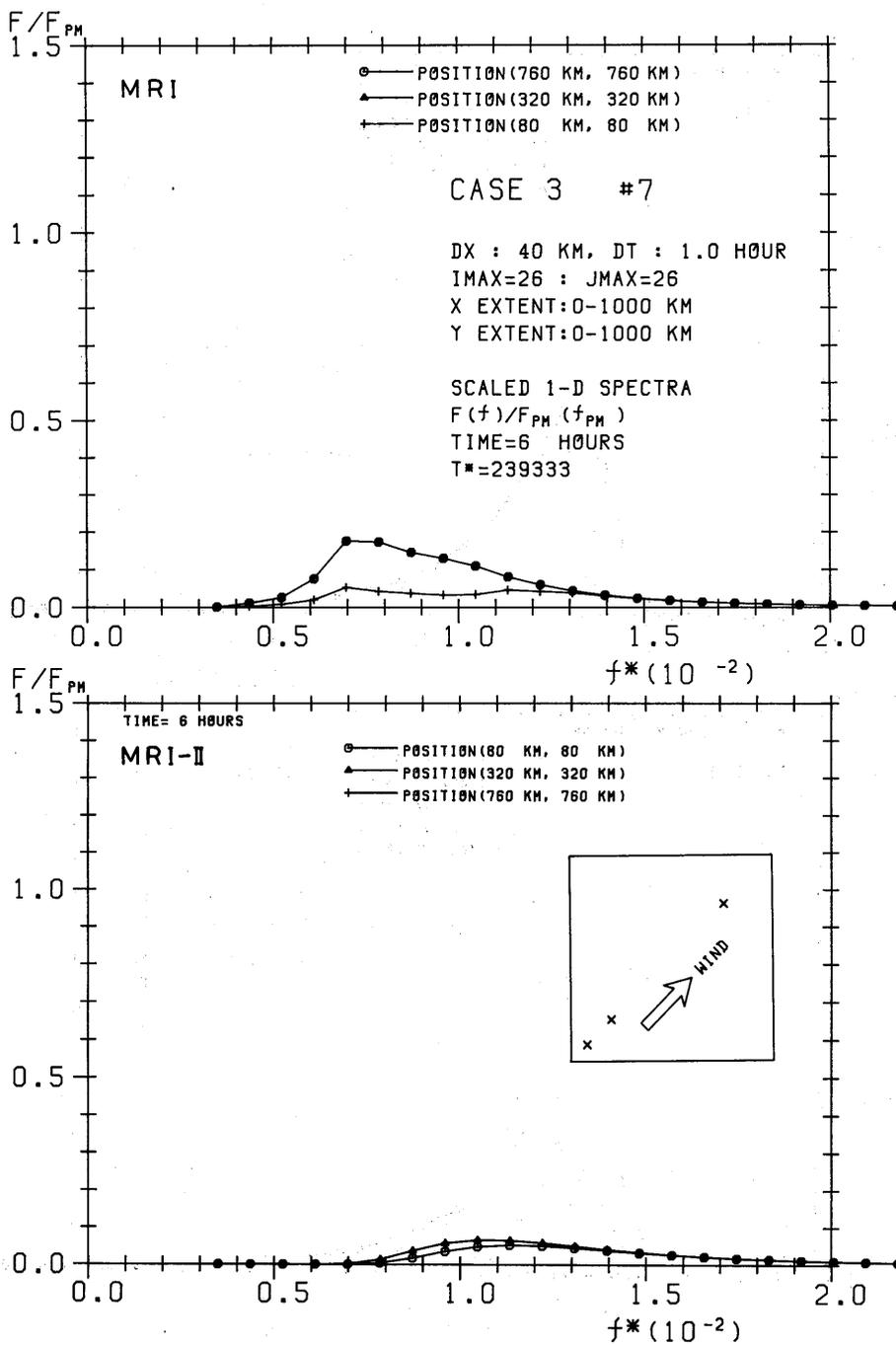


Fig. 38-0-0 scaled 1-D spectrum $F(f)/F_{PM}(f_{PM})$ vs. f^* for $T=6$ hours and points A, B, and D

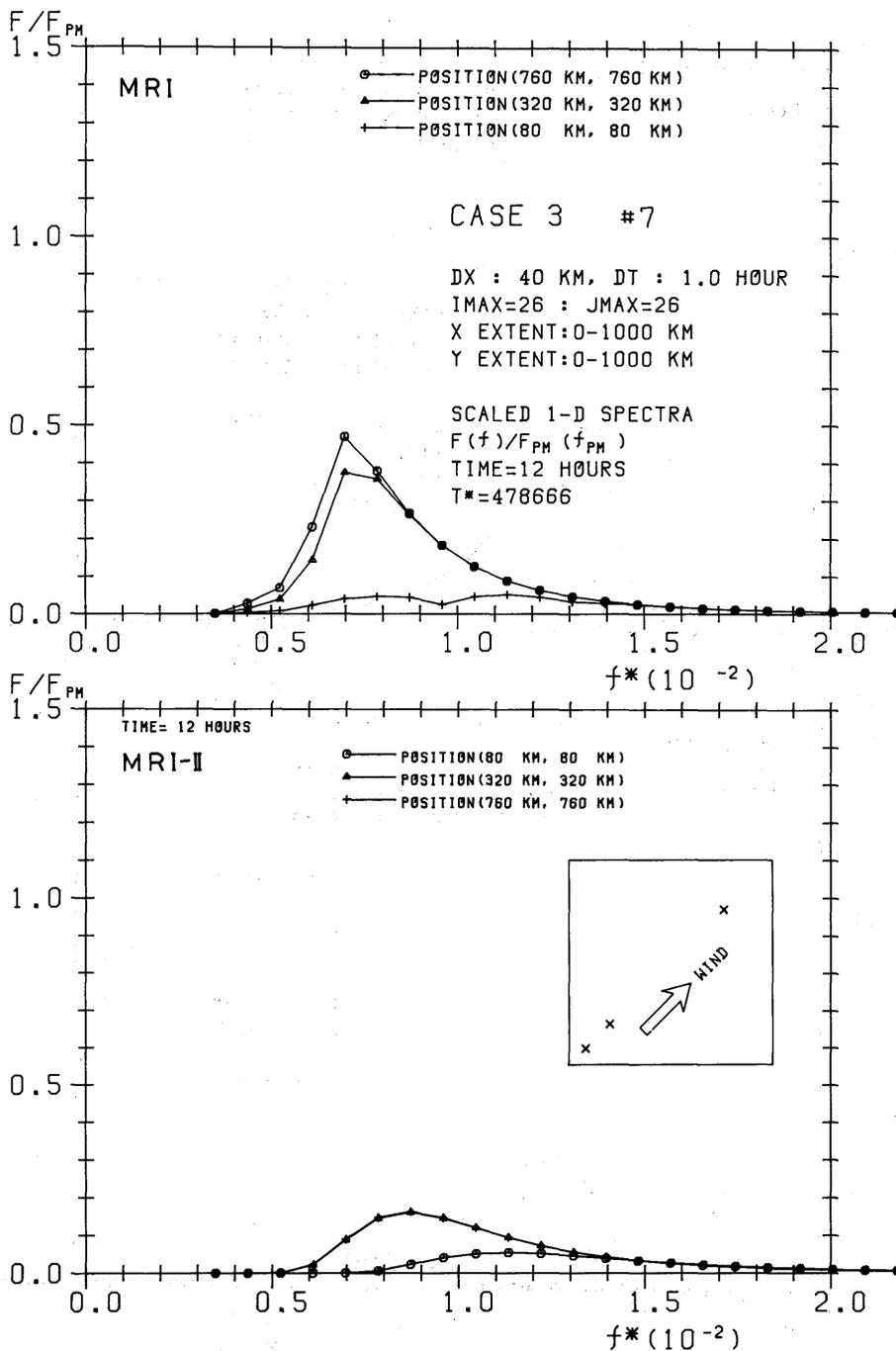


Fig. 39-0-0 scaled 1-D spectrum $F(f)/F_{PM}(f_{PM})$ vs. f^* for $T=12$ hours and points A, B, and D

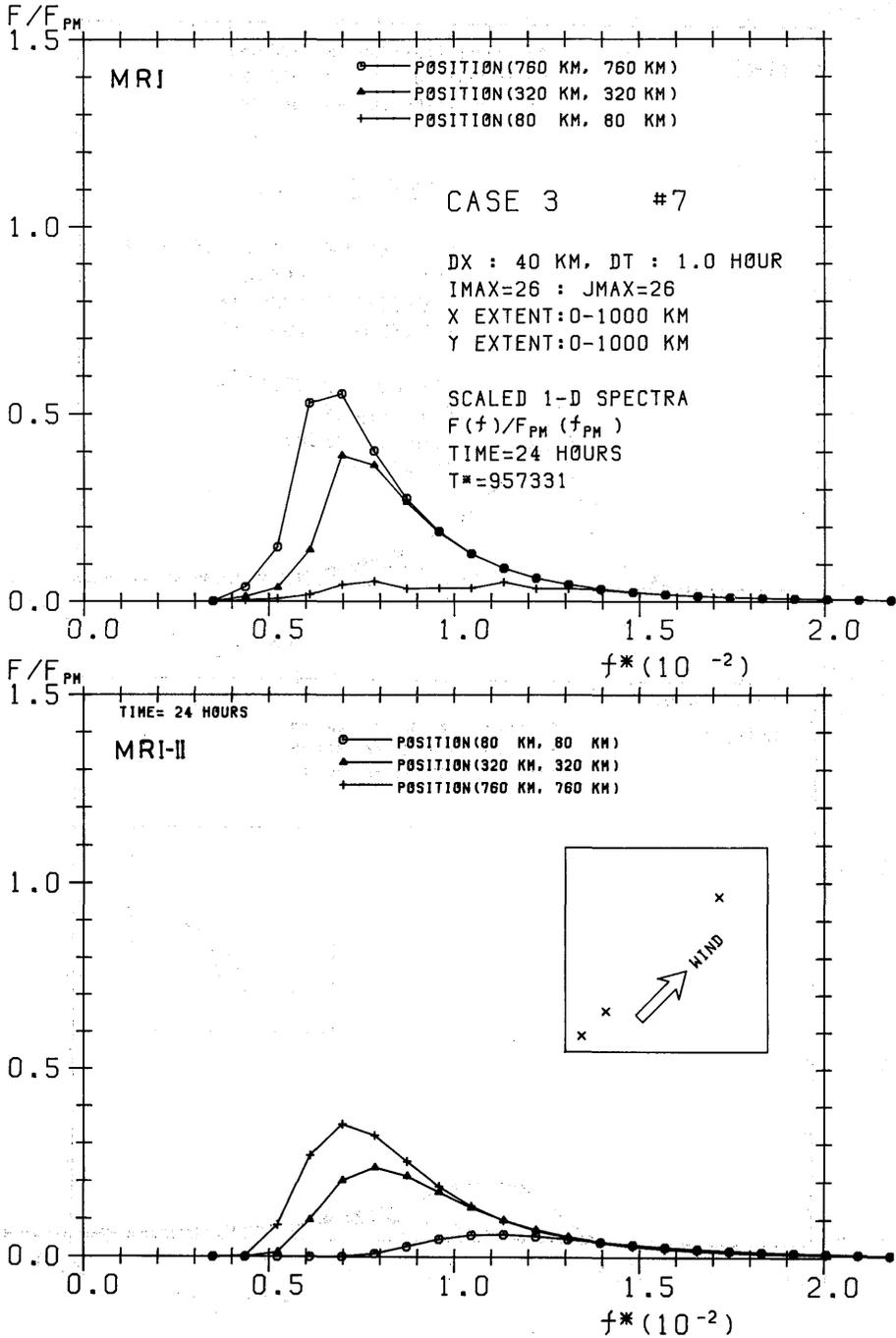


Fig. 40-0-0 scaled 1-D spectrum $F(f)/F_{PM}(f_{PM})$ vs. f^* for $T=24$ hours and points A, B, and D

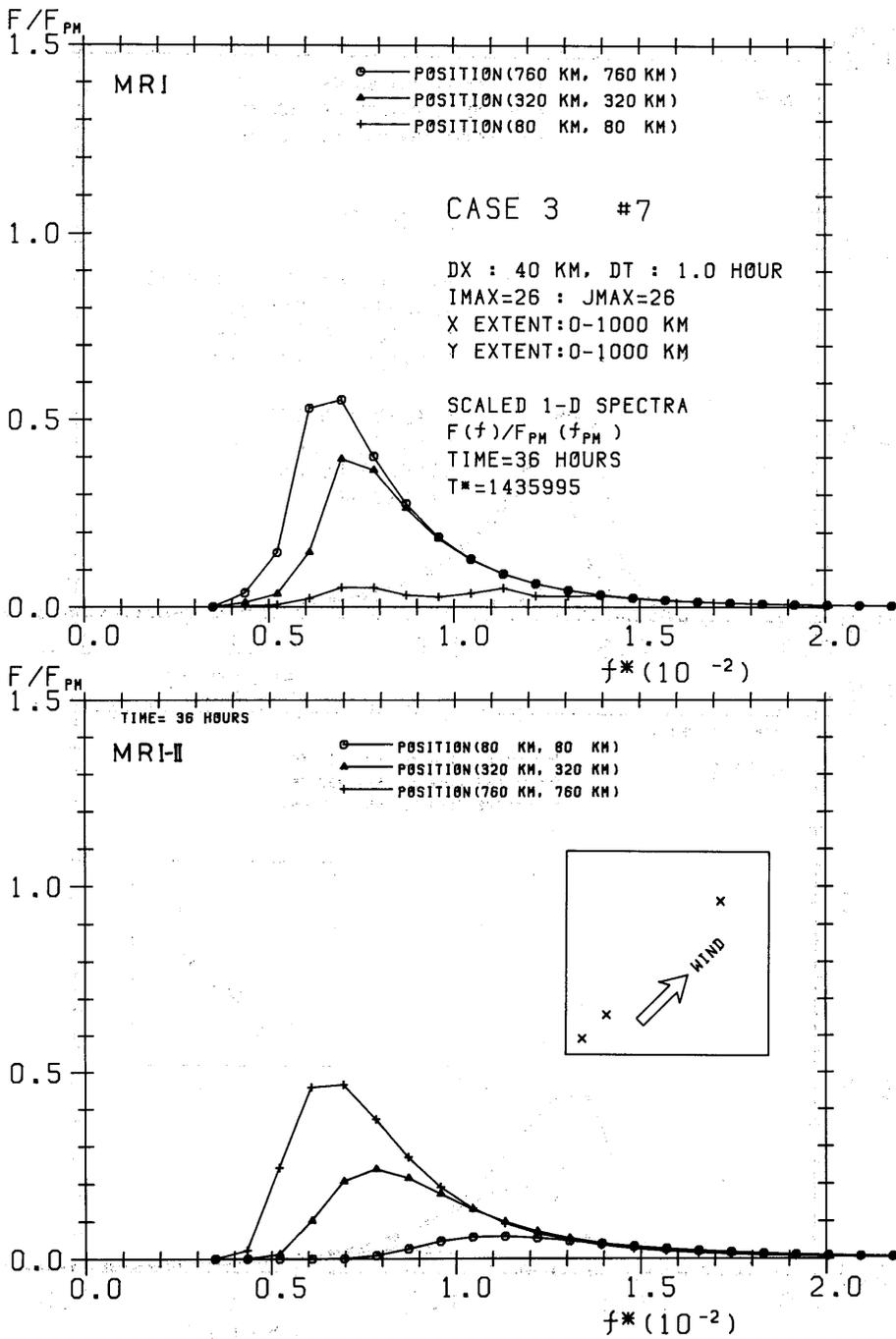


Fig. 41-0-14 scaled 1-D spectrum $F(f)/F_{PM}(f_{PM})$ vs. f^* for $T=36$ hours and points A, B, and D

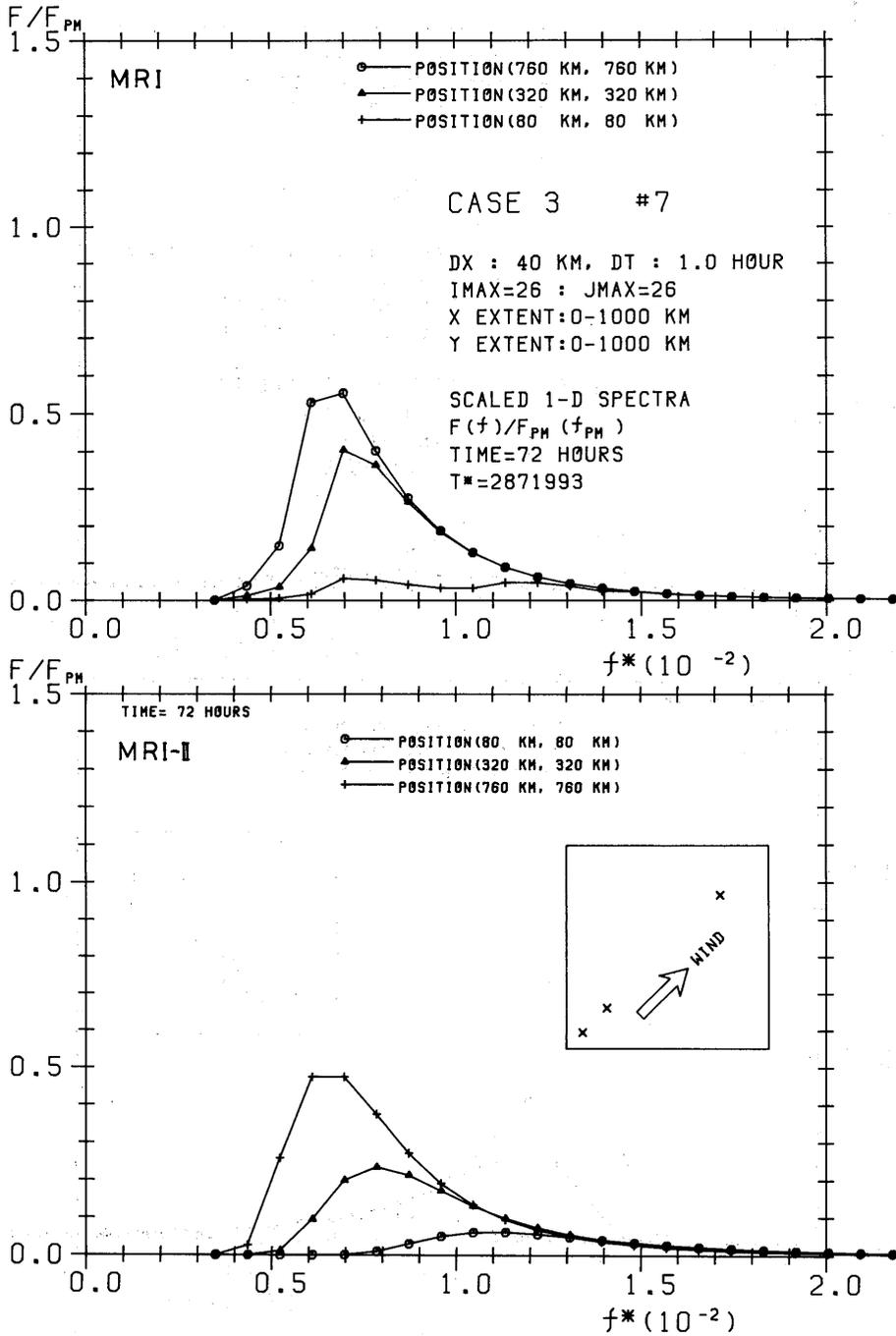


Fig. 42-0-0 scaled 1-D spectrum $F(f)/F_{PM}(f_{PM})$ vs. f^* for $T=72$ hours and points A, B, and D

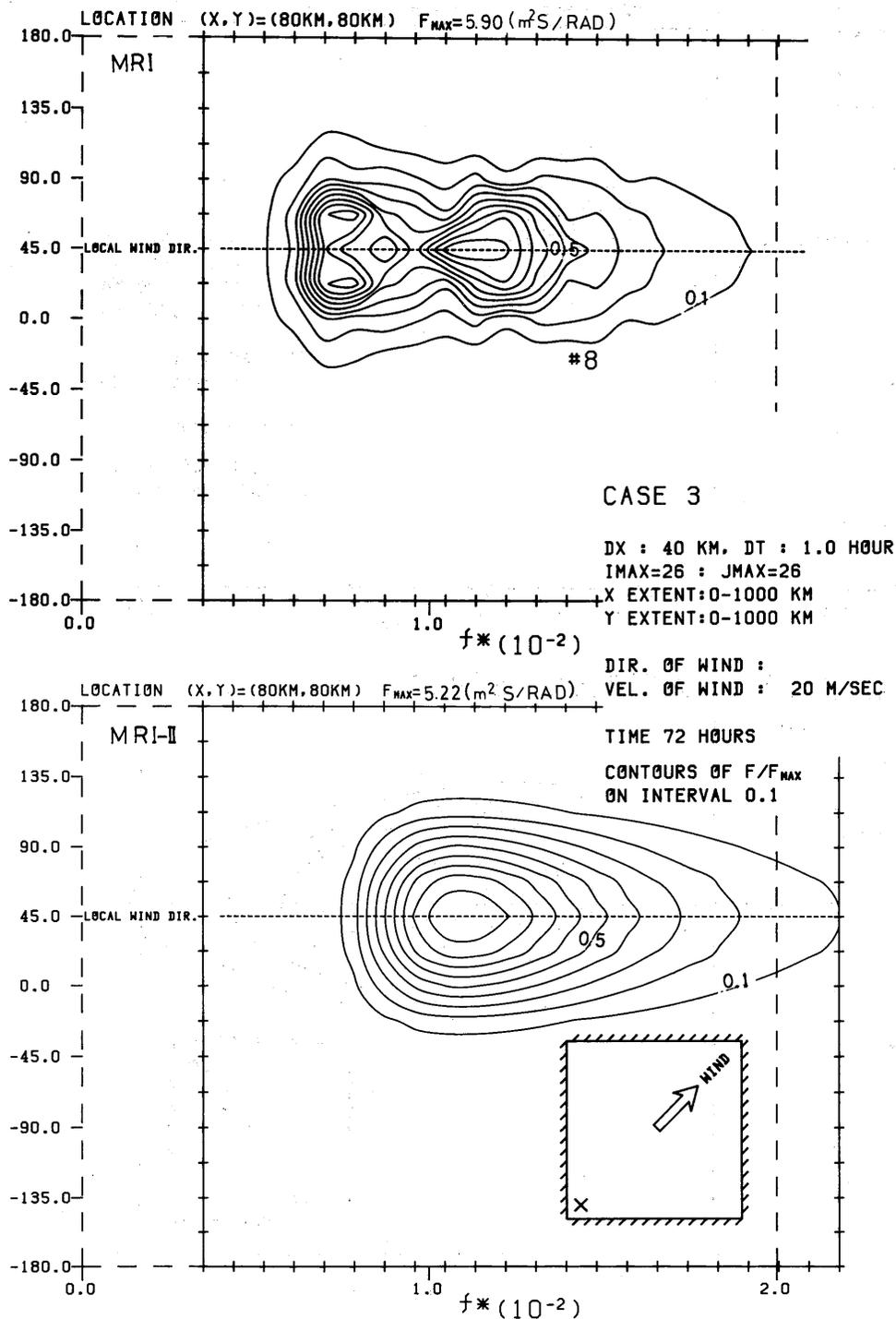


Fig. 43-0-15 scaled 2-D spectrum $F(f,\theta)/F(f,\theta)_{MAX}$ for $T=72$ hrs and point (80,80)

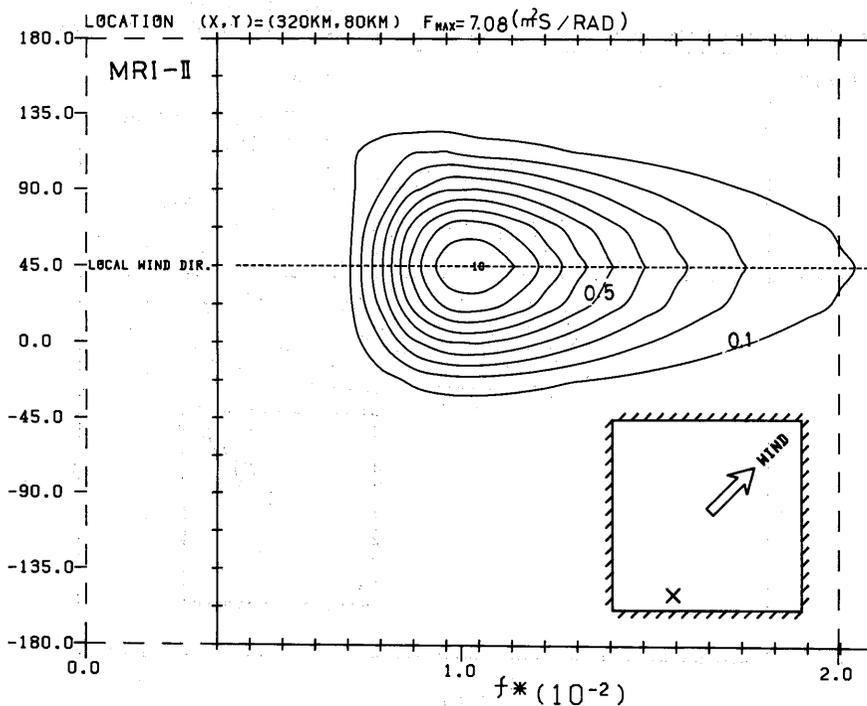
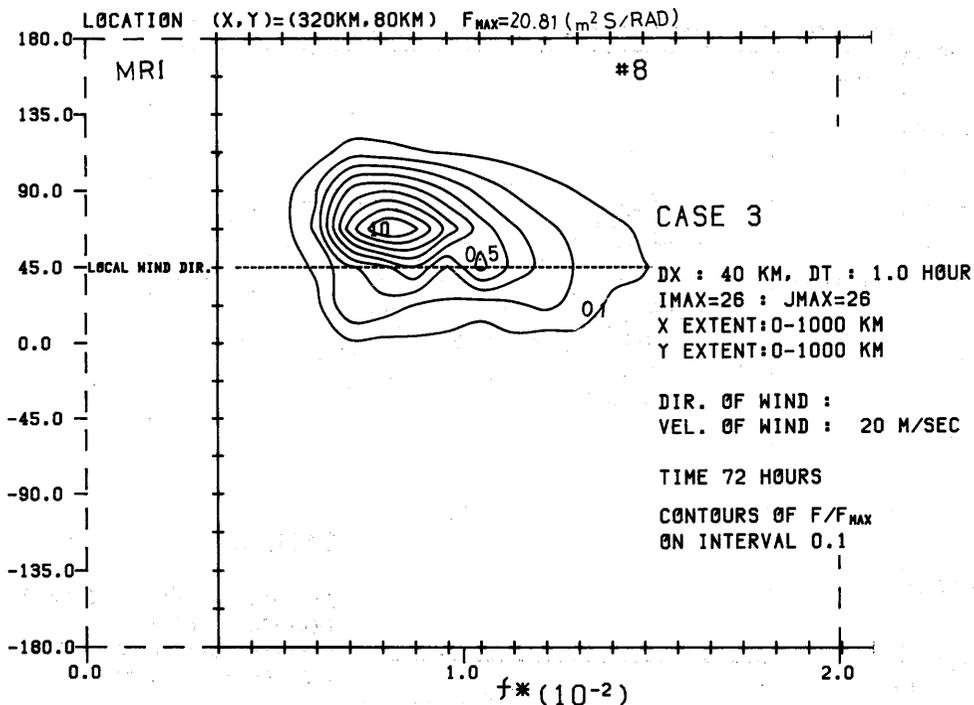


Fig. 44-0-0. scaled 2-D spectrum $F(f, \theta) / F(f, \theta)_{MAX}$ for $T=72$ hrs and point (320,80)

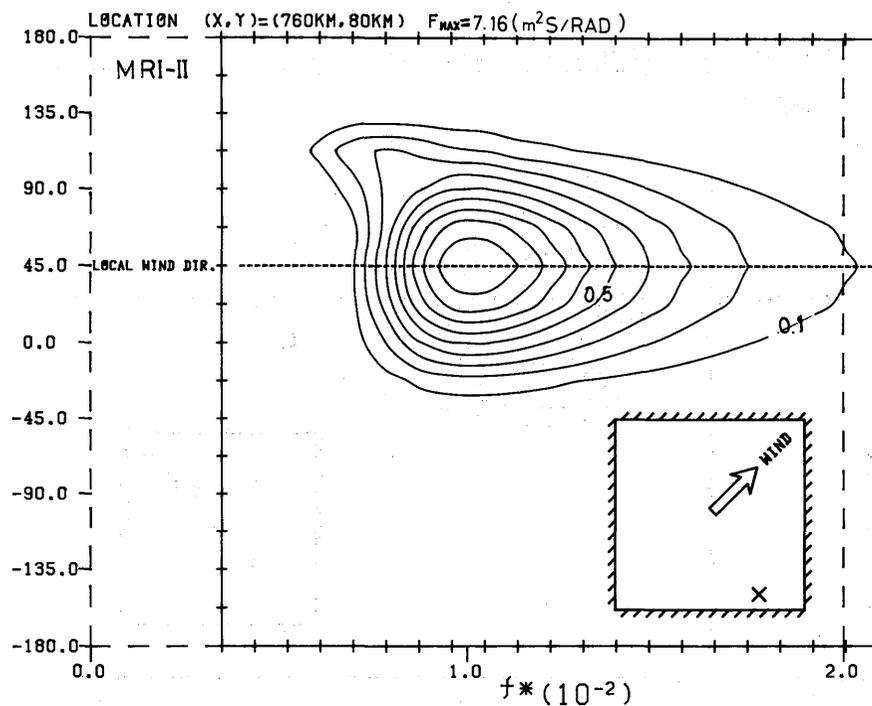
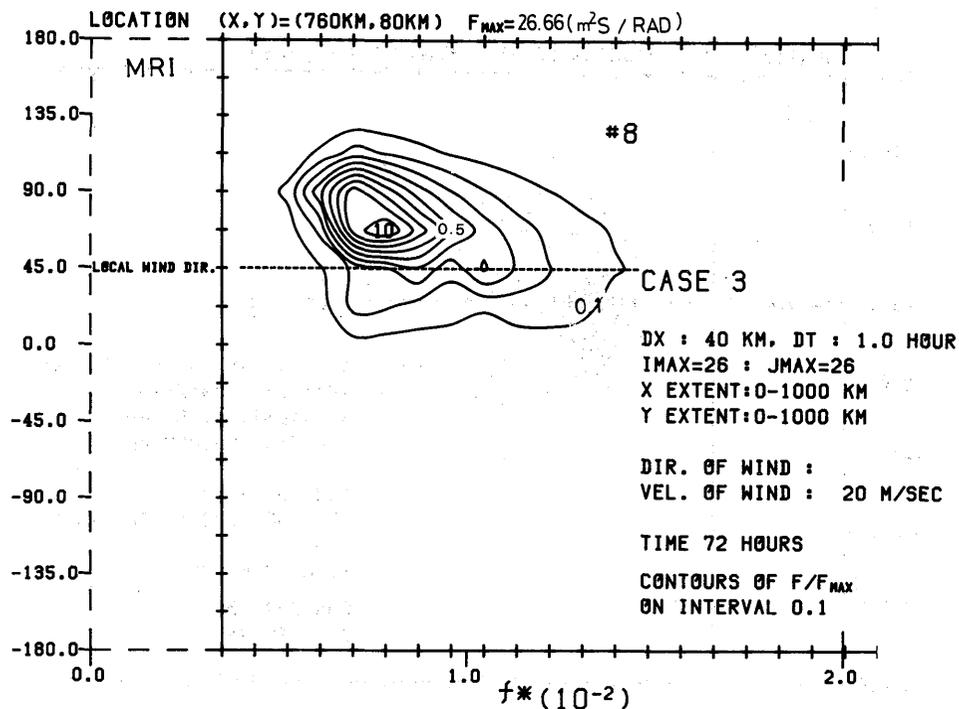


Fig. 45-8.4-16 scaled 2-D spectrum $F(f,\theta)/F(f,\theta)_{MAX}$ for $T=72$ hrs and point (760,80)

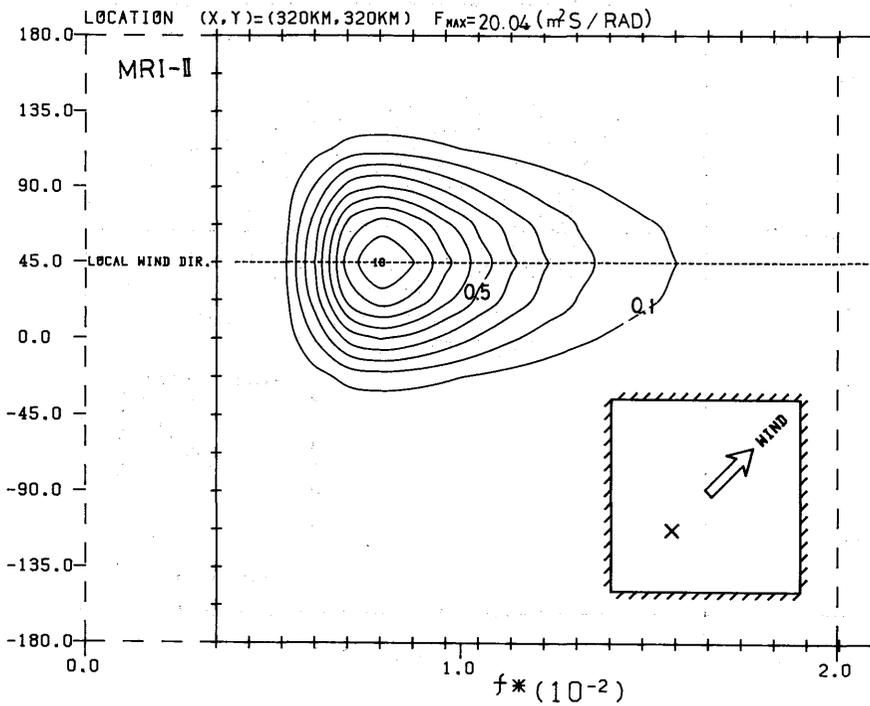
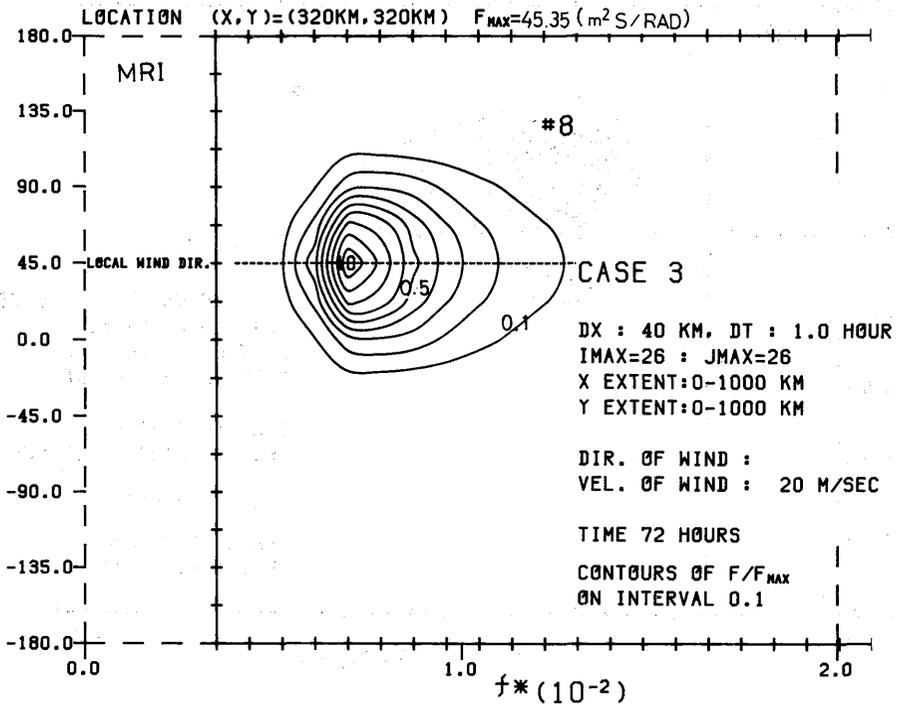


Fig. 46-0-0 scaled 2-D spectrum $F(f, \theta)/F(f, \theta)_{MAX}$ for $T=72$ hrs and point (320,320)

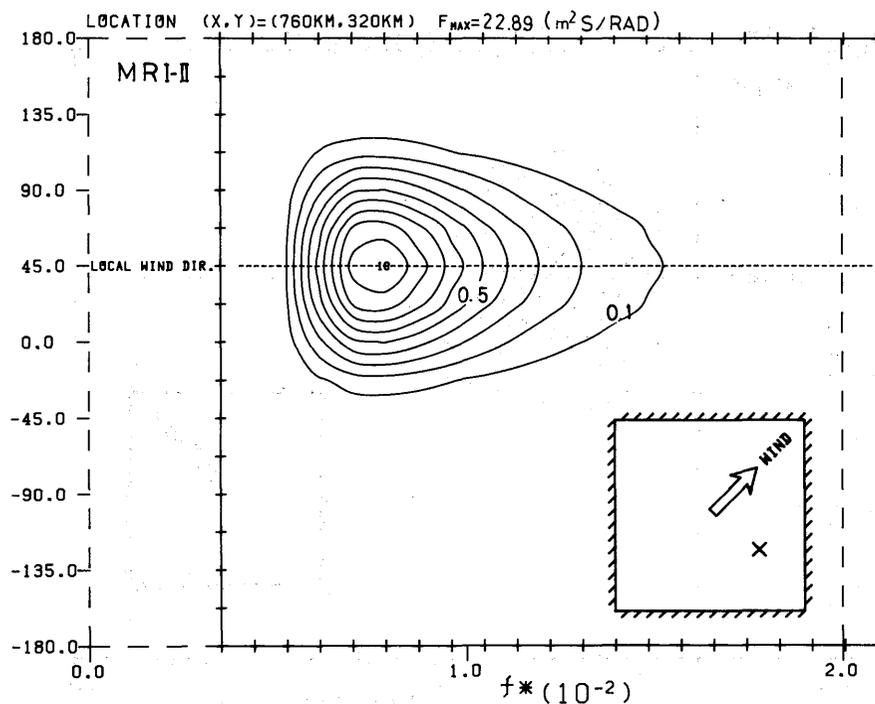
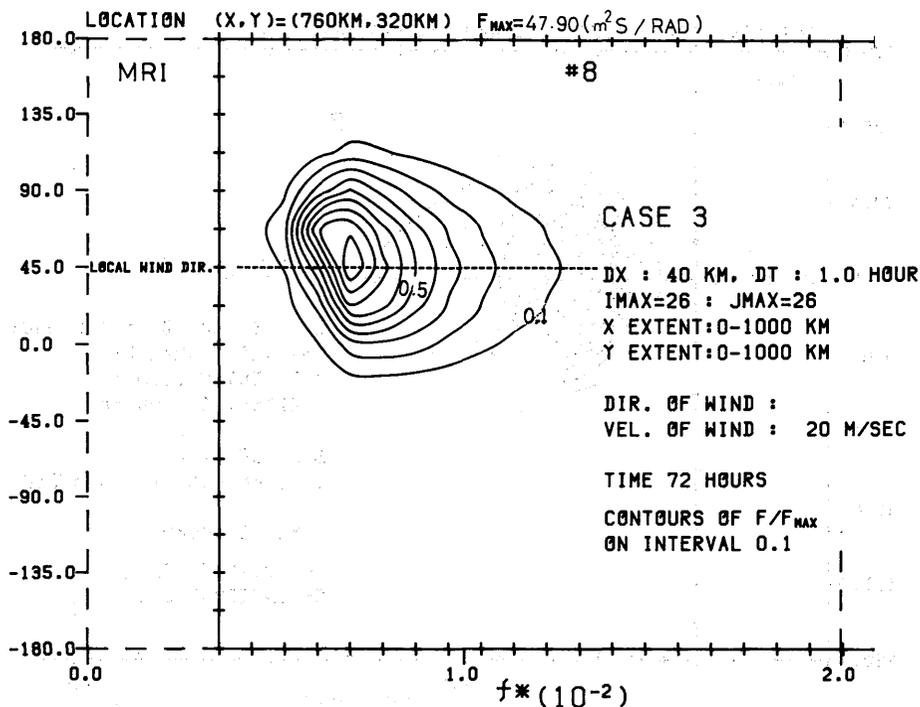


Fig. 47-0-17 scaled 2-D spectrum $F(f,\theta)/F(f,\theta)_{MAX}$ for $T=72$ hrs and point (760,320)

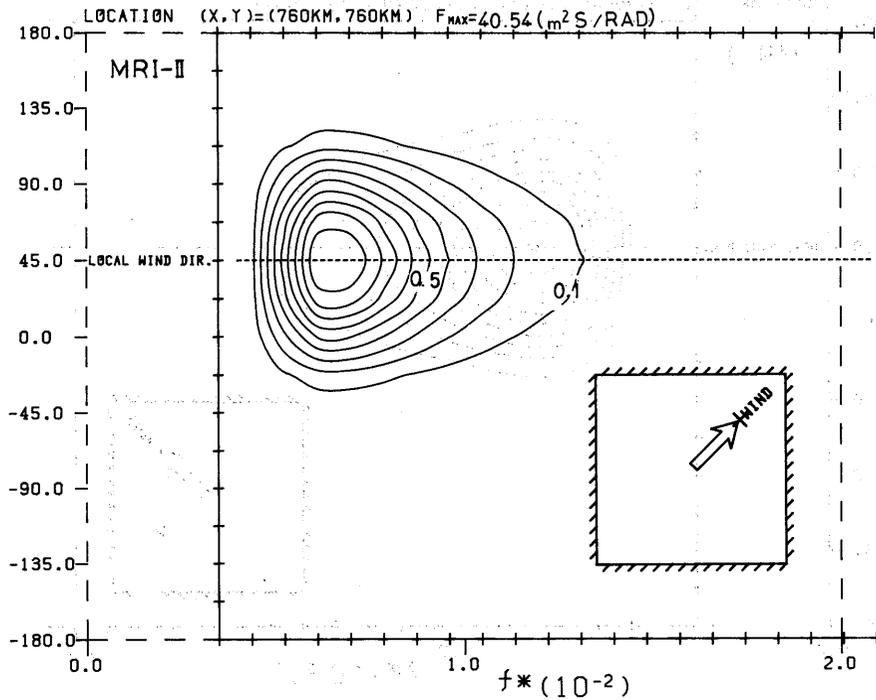
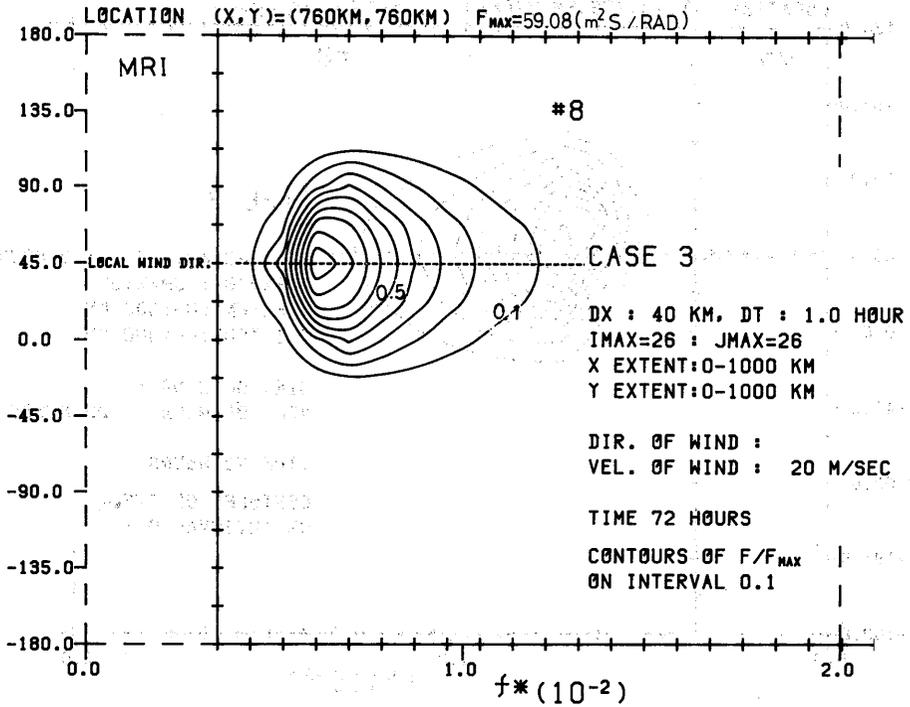


Fig. 48-0-0 scaled 2-D spectrum $F(f, \theta) / F(f, \theta)_{MAX}$ for $T = 72$ hrs and point (760, 760)

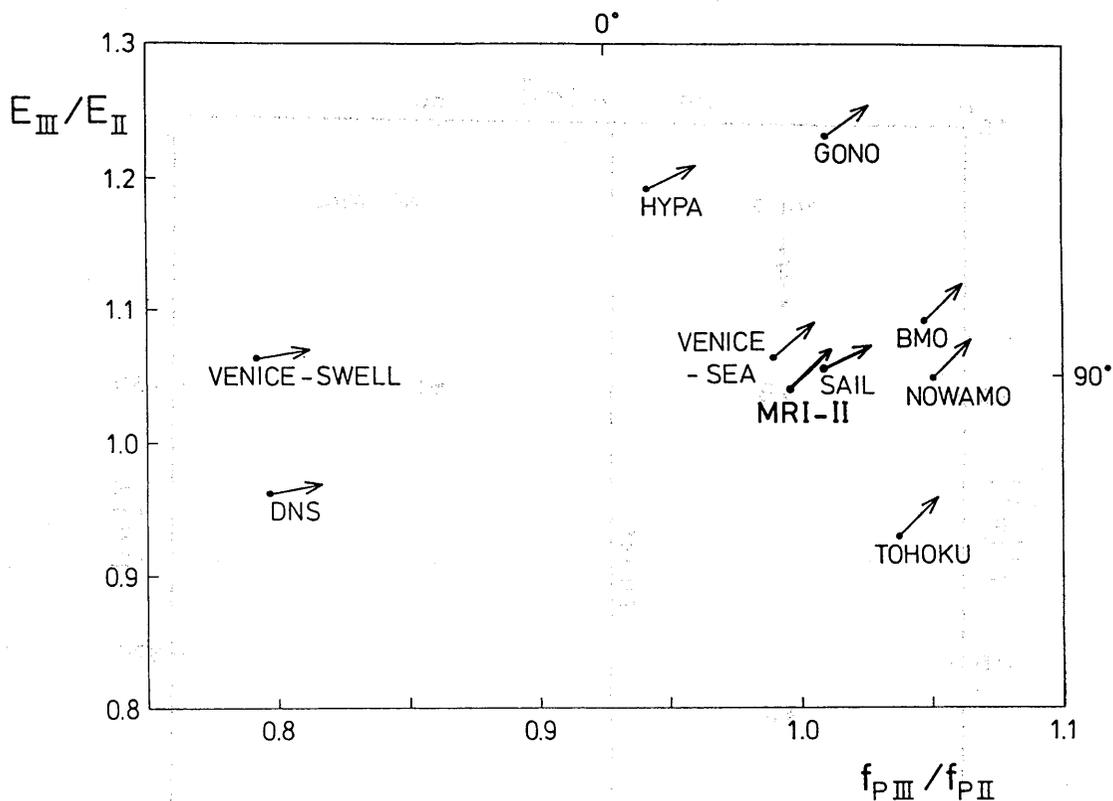


Fig. 49-8.5-0 location of models in the E_{III}/E_{II} vs. $f_{P_{III}}/f_{P_{II}}$ parameter plane at point F (MRI is not shown, as the peak windsea frequency was not well defined for Case II for the small fetch), where indices III and II refer to Case III and Case II for the same fetch.